NEUTRINO MASS AND MIXING PARAMETERS: A SHORT REVIEW

G.L. Fogli, E. Lisi [a], A. Marrone, A. Palazzo, A.M. Rotunno
Dipartimento di Fisica and Sezione INFN di Bari,
Via Amendola 173, 70126 Bari, Italy

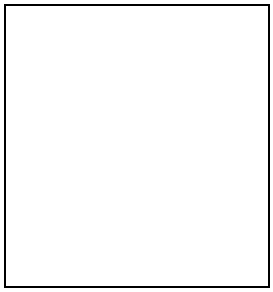

We present a brief review of the current status of neutrino mass and mixing parameters, based on a comprehensive phenomenological analysis of neutrino oscillation and non-oscillation searches, within the standard three-neutrino mixing framework.

1 Introduction

There is compelling experimental evidence [1] that the three known neutrino states with definite flavor ν_α ($\alpha = e, \mu, \tau$) are linear combinations of states with definite mass ν_i ($i = 1, 2, 3$), and that the Hamiltonian of neutrino propagation in vacuum [2] and matter [3] does not commute with flavor. The evidence for flavor nonconservation (i.e., "neutrino oscillations") comes from a series of experiments performed during about four decades of research with very different neutrino beams and detection techniques: the solar neutrino [4] experiments Homestake [5], Kamiokande [6], SAGE [7], GALLEX-GNO [8,9], Super-Kamiokande (SK) [10] and the Sudbury Neutrino Observatory (SNO) [11,12,13]; the long-baseline reactor neutrino experiment KamLAND [14,15]; the atmospheric neutrino experiments Super-Kamiokande [16,17], MACRO [18], and Soudan-2 [19]; and the long-baseline accelerator neutrino experiment KEK-to-Kamioka (K2K) [20,21].

Together with the null results from the CHOOZ [22] short-baseline reactor experiment, the above oscillation data provide stringent constraints on the neutrino mixing matrix, on the splittings between squared neutrino masses, and on matter effects. The absolute neutrino masses are being probed by different, non-oscillation searches: beta decay experiments [23], neutrinoless double beta decay searches ($0\nu2\beta$) [24,25], and precision cosmology [26,27,28,29,30]. Current non-oscillation data provide only upper limits on neutrino masses, with the only exception of the

[a] Speaker. E-mail: eligio.lisi@ba.infn.it

Heidelberg-Moscow $0\nu2\beta$ experiment [31], whose claimed signal implies a lower bound on neutrino masses.

Basically all the data are consistent with the simplest extension of the standard electroweak model needed to accommodate nonzero neutrino masses and mixings, namely, with a scenario where the three known flavor states $\nu_{e,\mu,\tau}$ are mixed with only three mass states $\nu_{1,2,3}$, no other states or new neutrino interactions being needed. This "standard three-neutrino framework" (as recently reviewed, e.g., in [32], where further references can be found) appears thus as a new paradigm of particle and astroparticle physics, which will be tested, refined, and possibly challenged by a series of new, more sensitive experiments planned for the next few years or even for the next decades [33]. The first challenge might actually come very soon from the running MiniBooNE experiment [34], which is probing the only piece of data at variance with the standard three-neutrino framework, namely, the controversial result of the Liquid Scintillator Neutrino Experiment (LSND) [35].

In this short review we focus on the current status of the standard three-neutrino framework and on the neutrino mass and mixing parameters which characterize it. The parameters are defined as follows. The unitary mixing matrix U, in terms of one-particle neutrino states $|\nu\rangle$, is defined as (see, e.g., [1]),

$$|\nu_\alpha\rangle = \sum_{i=1}^{3} U^*_{\alpha i} |\nu_i\rangle \ . \tag{1}$$

A common parameterization for the matrix U is:

$$U = O_{23} \Gamma_\delta O_{13} \Gamma_\delta^\dagger O_{12} \ , \tag{2}$$

where the O_{ij}'s are real Euler rotations with angles $\theta_{ij} \in [0, \pi/2]$, while Γ_δ embeds a CP-violating phase $\delta \in [0, 2\pi]$,

$$\Gamma_\delta = \mathrm{diag}(1, 1, e^{+i\delta}) \ . \tag{3}$$

By considering $\Gamma_\delta O_{13} \Gamma_\delta^\dagger$ as a single (complex) rotation, this parametrization coincides with the one recommended [together with Eq. (1)] in the Review of Particle Properties [1].

For the sake of simplicity, the phase δ will not be considered in full generality hereafter. Numerical examples will refer only to the two inequivalent CP-conserving cases, namely, $e^{i\delta} = \pm 1$. In these two cases, the mixing matrix takes a real form $U_{\rm CP}$,

$$U_{\rm CP} = \begin{pmatrix} c_{13}c_{12} & s_{12}c_{13} & \pm s_{13} \\ -s_{12}c_{23} \mp s_{23}s_{13}c_{12} & c_{23}c_{12} \mp s_{23}s_{13}s_{12} & s_{23}c_{13} \\ s_{23}s_{12} \mp s_{13}c_{23}c_{12} & -s_{23}c_{12} \mp s_{13}s_{12}c_{23} & c_{23}c_{13} \end{pmatrix} \ , \tag{4}$$

where the upper (lower) sign refers to $\delta = 0$ ($\delta = \pi$). The two cases are formally related by the replacement $s_{13} \to -s_{13}$.

The three-neutrino mass spectrum $\{m_i\}_{i=1,2,3}$ is formed by a "doublet" of relatively close states and by a third "lone" neutrino state, which may be either heavier than the doublet ("normal hierarchy," NH) or lighter ("inverted hierarchy," IH). Here, the lightest (heaviest) neutrino in the doublet is called ν_1 (ν_2), so that their squared mass difference is

$$\delta m^2 = m_2^2 - m_1^2 > 0 \tag{5}$$

by convention. The lone state is then labeled as ν_3, and the physical sign of $m_3^2 - m_{1,2}^2$ distinguishes NH from IH.

Concerning the second independent squared mass difference Δm^2, we define it as [32,36]

$$\Delta m^2 = \left| m_3^2 - \frac{m_1^2 + m_2^2}{2} \right| \ , \tag{6}$$

so that the two hierarchies (NH and IH) are simply related by the transformation $+\Delta m^2 \to -\Delta m^2$. The largest and next-to-largest squared mass gaps are given $\Delta m^2 \pm \delta m^2/2$ in both cases. More precisely, the squared mass matrix M^2 reads, in such convention,

$$M^2 = \mathrm{diag}(m_1^2, m_2^2, m_3^2) = \frac{m_2^2 + m_1^2}{2}\,\mathbf{1} + \mathrm{diag}\left(-\frac{\delta m^2}{2}, +\frac{\delta m^2}{2}, \pm\Delta m^2\right) \,, \tag{7}$$

where the upper (lower) sign refers to normal (inverted) hierarchy.

In the previous equation, the term proportional to the unit matrix $\mathbf{1}$ is irrelevant in neutrino oscillations, while it matters in observables sensitive to the absolute neutrino mass scale, such as in β-decay and precision cosmology. In particular, β-decay experiments are sensitive to the so-called effective electron neutrino mass m_β,

$$m_\beta = \left[\sum_i |U_{ei}|^2 m_i^2\right]^{\frac{1}{2}} = \left[c_{13}^2 c_{12}^2 m_1^2 + c_{13}^2 s_{12}^2 m_2^2 + s_{13}^2 m_3^2\right]^{\frac{1}{2}} \,, \tag{8}$$

as far as the single ν_i mass states are not experimentally resolvable. On the other hand, precision cosmology is sensitive, to a good approximation (up to small hierarchy-dependent effects which may become important in next-generation precision measurements [37]) to the sum of neutrino masses Σ [30],

$$\Sigma = m_1 + m_2 + m_3 \,. \tag{9}$$

Finally, if neutrinos are indistinguishable from their antiparticles (i.e., if they are Majorana rather than Dirac neutrinos), the mixing matrix U acquires a (diagonal) extra factor

$$U \to U \cdot U_M \,, \tag{10}$$

containing Majorana phases ϕ_i, which are irrelevant in oscillations but not in neutrinoless double beta decay ($0\nu2\beta$). Using the parametrization

$$U_M = \mathrm{diag}\left(1, \mathrm{e}^{\frac{\mathrm{i}}{2}\phi_2}, \mathrm{e}^{\frac{\mathrm{i}}{2}(\phi_3 + 2\delta)}\right) \,, \tag{11}$$

the expression of the effective Majorana mass $m_{\beta\beta}$ probed in $0\nu2\beta$ experiments [1] takes the form:

$$m_{\beta\beta} = \left|\sum_i U_{ei}^2 m_i\right| = \left|c_{13}^2 c_{12}^2 m_1 + c_{13}^2 s_{12}^2 m_2 e^{i\phi_2} + s_{13}^2 m_3 e^{i\phi_3}\right| \,. \tag{12}$$

Finally, we remark that the constraints on the neutrino oscillation parameters shown hereafter have been obtained by fitting accurate theoretical predictions to a large set of experimental data, through either least-square or maximum-likelihood methods. In both cases, parameter estimations reduce to finding the minimum of a χ^2 function and to tracing iso-$\Delta\chi^2$ contours around it. We adopt the convention used in [1] and call "region allowed at $n\sigma$" the subset of the parameter space obeying the inequality

$$\Delta\chi^2 \leq n^2 \,. \tag{13}$$

The projection of such allowed region onto each single parameter provides the $n\sigma$ bound on such parameter. In particular, we shall also directly use the relation $\sqrt{\Delta\chi^2} = n$ to derive allowed parameter ranges at n standard deviations. Numerical results and figures are taken from the recent review [32] (to which the reader is referred for details), which also makes use of results from Refs. [38,39]. For previous reviews on neutrino parameters see, e.g., Refs. [40,41,42,43,44,45,46,47].

2 Constraints on $(\delta m^2, \sin^2\theta_{12}, \sin^2\theta_{13})$ from solar+KamLAND data

It is well known that the angle θ_{13} is relatively small and possibly zero. For $\theta_{13} = 0$, both solar and (long-baseline) reactor neutrino oscillations depend solely on the parameters $(\delta m^2, \theta_{12})$. Figure 1 shows the current constraints on such parameters from a global analysis of all the available solar neutrino data [32] and of KamLAND data [38], both separately and in combination. Although (at 3σ) multiple solutions can explain KamLAND data, the combination with solar data provides a well-defined and unique solution at large mixing angle (LMA) in the mass-mixing parameter space. The identification of such solution represents one of the most impressive recent advances in neutrino physics.

Further progress can be expected in narrowing the parameter space in Fig. 1. The δm^2 uncertainty is currently dominated by the KamLAND observation of half-period of oscillations [14] and can be improved with higher statistics [15]. The $\sin^2\theta_{12}$ uncertainty is instead dominated by the SNO ratio of charged-to-neutral current (CC/NC) event rates, which can also be improved with future data [13].

The current solar LMA solution, as compared with results prior to the complete SNO-II data set [13], is slightly shifted toward larger values of $\sin^2\theta_{12}$ and allows higher values of δm^2. [Our current best-fit point for solar data only is at $\delta m^2 = 6.3 \times 10^{-5}$ eV^2 and $\sin^2\theta_{12} = 0.314$.] This trend is substantially due to the larger value of the CC/NC ratio measured in the complete SNO II phase (0.34 [12,13]) with respect to the previous central value (0.31 [11]). We also find that the SNO-II charged-current spectral data [12] contribute to allow slightly higher values of δm^2 with respect to older results.

For $\theta_{13} > 0$, the solar and KamLAND ν parameter space is spanned by $(\delta m^2, \sin^2\theta_{12}, \sin^2\theta_{13})$. Figure 2 shows the current 2σ bounds in such space (both separately and in combination) in each of the three coordinate planes. Remarkably, both solar and KamLAND data are consistent with θ_{13} being small (~ 0 at best-fit), in agreement with independent atmospheric, accelerator and short-baseline reactor data (see the next section). The combined upper bound on $\sin^2\theta_{13}$ in Fig. 2 is at the interesting level of $\sim 5\%$.

3 Constraints on $(\Delta m^2, \sin^2\theta_{23}, \sin^2\theta_{13})$ from SK$_{\rm ATM}$+K2K+CHOOZ data

In the limit $\delta m^2/\Delta m^2 \ll 1$ (one-dominant-mass-scale approximation), the leading parameters in atmospheric and long-baseline accelerator searches are $(\Delta m^2, \sin^2\theta_{23}, \sin^2\theta_{13})$. Subleading effects induced by $\delta m^2 \neq 0$ (i.e., LMA effects in terrestrial neutrino oscillations [48,49,50]) are present, however, even for $\theta_{13} \neq 0$ [51]. In accurate calculations, it is worthwhile to include such effects numerically, e.g., by fixing $(\delta m^2, \sin^2\theta_{12})$ at their best-fit value in Fig. 1 in a full three-flavor analysis of atmospheric and K2K data, as done in the following two figures.

Figure 3 shows, for $\theta_{13} = 0$, the results of our analysis of SK (atmospheric) and K2K data, both separately and in combination. The K2K constraints are octant-symmetric and relatively weak in $\sin^2\theta_{23}$, while they contribute appreciably to reduce the overall Δm^2 uncertainty. The SK atmospheric neutrino contraints are instead strong on both mass and mixing parameters, and also slightly asymmetrical [51] in $\sin^2\theta_{23}$. Unfortunately, current data are not accurate enough to promote this slight asymmetry to a real θ_{23}-octant discrimination. However, it is not excluded that future, high-statistics atmospheric neutrino data might be able to do so, if θ_{23} is not too close to $\pi/4$ [52]. Such possible θ_{23} octant asymmetry, together with a measurement of θ_{13}, is crucial for model building [53,54].

For $\theta_{13} > 0$, SK+K2K data are also sensitive, in principle, to the neutrino mass hierarchy [sign$(\pm\Delta m^2) = \pm 1$] and to the CP parity [$\cos\delta = \pm 1$]. However, the dependence is very small within the CHOOZ bounds on θ_{13} (see, e.g., Ref. [32] and references therein), and thus it makes sense to marginalize the SK+K2K+CHOOZ χ^2 function with respect to hierarchy and CP parity.

The results are shown in Fig. 4, in terms of the projections of the $(\Delta m^2, \sin^2\theta_{23}, \sin^2\theta_{13})$ region allowed at 1, 2, and 3σ onto each of the coordinate planes (with LMA effects included). The best fit is reached for nonzero θ_{13} (mainly due to a slight preference of low-energy atmospheric data for ν_e event appearance), but $\theta_{13} = 0$ is allowed within less than 1σ. The preferred value of $\sin^2\theta_{23}$ remains slightly below maximal mixing. The best-fit value of Δm^2 is 2.4×10^{-3} eV^2. Notice that the correlations among the three parameters in Fig. 4 are very weak.

4 Global constraints on oscillation parameters

The results of the global analysis of solar+KamLAND data (Sec. 2) and of SK+K2K+CHOOZ data (Sec. 3) can now be merged to provide our best estimates of the five neutrino oscillation parameters $(\delta m^2, \Delta m^2, \theta_{12}, \theta_{13}, \theta_{23})$, marginalized over the 2×2 cases with different mass hierarchies and CP parities (which are physically different but phenomenologically indistinguishable at present). The bounds will be directly shown in terms of the "number of sigmas", corresponding to the function $(\Delta\chi^2)^{1/2}$ for each parameter.

Figure 5 shows our global bounds on $\sin^2\theta_{13}$, as coming from all data (solid line) and from the following partial data sets: KamLAND (dotted), solar (dot-dashed), solar+KamLAND (short-dashed) and SK+K2K+CHOOZ (long-dashed). Only the latter set, as observed before, gives a weak indication for nonzero θ_{13}. Interestingly, solar+KamLAND data are now sufficiently accurate to provide bounds which are not much weaker than the dominant SK+K2K+CHOOZ ones, also because the latter slightly prefer $\theta_{13} > 0$ as best fit, while the former do not.

Figure 6 shows our global bounds on the four mass-mixing parameters which present both upper and lower limits with high statistical significance. Notice that the accuracy of the parameter estimate is already good enough to lead to almost "linear" errors, especially for δm^2 and $\sin^2\theta_{12}$. For Δm^2 and $\sin^2\theta_{23}$, such "linearity" is somewhat worse in the region close to the best fit (say, within $\pm 1\sigma$), and thus 2σ (or 3σ) errors should be taken as reference.

5 Non-oscillation data and their interplay with oscillation constraints

Since oscillation data fix the mass splittings δm^2 and Δm^2, the observables sensitive to absolute neutrino masses $(m_\beta, m_{\beta\beta}, \Sigma)$ are higly correlated with each other, both in normal and in inverted hierarchy: typically, when one increases the other also increases. Therefore, upper bounds on any of them translate into upper bounds on the others. However, the upper bounds on m_β are currently weak (a few eV) [23], and the relevant discussion can be limited to $(m_{\beta\beta}, \Sigma)$ at present.

Figure 7 shows the impact of all the available non-oscillation data, taken at face value, in the parameter space $(m_{\beta\beta}, \Sigma)$, at the 2σ level. The horizontal band is allowed by the positive $0\nu2\beta$ experimental claim [31] equipped with the nuclear uncertainties of [55] as described in [32]. The slanted bands (for normal and inverted hierarchy) are allowed by all other neutrino data, i.e., by the combination of neutrino oscillation constraints (from Figs. 5 and 6) and of astrophysical and cosmological constraints from Cosmic Microwave Background (CMB) [27], large scale structures from galaxy surveys (2dF) [56], and small scale structures from Lyman α forest data [57], as described in [39]. The tight cosmological upper bound on Σ prevents the overlap between the slanted and horizontal bands at 2σ, indicating that no global combination of oscillation and non-oscillation data is possible in the sub-eV range. The "discrepancy" is now even stronger than it was found in Ref. [39], due to the adoption of smaller $0\nu2\beta$ nuclear uncertainties [55]. It is premature, however, to derive any definite conclusion as to which piece of the data (or of the 3ν scenario) is "wrong" in this conflicting picture. E.g., by relaxing either the $0\nu2\beta$ lower bound or the Lyα data, global combinations are possible [32]. Further experimental and theoretical research is needed to clarify the interplay of absolute neutrino observables in the sub-eV range.

6 Summary and Conclusions

There is compelling evidence for neutrino flavor change driven by nonzero masses and mixing angles. Basically all oscillation data (with the only exception of LSND) are consistent within a three-neutrino framework. Within such framework, the global constraints from oscillation data can be summarized (see also Figs. 5 and 6 and Ref. [32]) through the following $\pm 2\sigma$ ranges (95% C.L.) for each parameter:

$$\sin^2\theta_{13} = 0.9^{+2.3}_{-0.9} \times 10^{-2} \ , \quad (14)$$

$$\delta m^2 = 7.92\,(1 \pm 0.09) \times 10^{-5}\ \mathrm{eV}^2 \ , \quad (15)$$

$$\sin^2\theta_{12} = 0.314\,(1^{+0.18}_{-0.15}) \ , \quad (16)$$

$$\Delta m^2 = 2.4\,(1^{+0.21}_{-0.26}) \times 10^{-3}\ \mathrm{eV}^2 \ , \quad (17)$$

$$\sin^2\theta_{23} = 0.44\,(1^{+0.41}_{-0.22}) \ . \quad (18)$$

Such ranges are marginalized over the four inequivalent cases $[\mathrm{sign}(\pm\Delta m^2)] \otimes [\cos\delta = \pm 1]$, i.e., over the two possible hierarchies and the two possible CP-conserving cases, which are currently undistinguishable. [Notice that the lower error on $\sin^2\theta_{13}$ is purely formal, and corresponds to the positivity constraints $\sin^2\theta_{13} > 0$.]

Concerning the observables sensitive to absolute masses (m_β, $m_{\beta\beta}$ and Σ), the situation is still unclear. Current constraints at the eV/sub-eV level are dominated by either upper bounds on Σ from cosmology or by the $0\nu 2\beta$ claim on $m_{\beta\beta}$, whose combination is not possible, however, at face value. Further studies and data are need to go beyond the general statement that neutrino masses should be smaller than ~ 1 eV, and to really explore the sub-eV range.

Within the three-neutrino scenario, it appears that the most important unsolved problems require probing θ_{13}, δ, the hierarchy, and the absolute neutrino masses. Needless to say, further experimental results or theoretical insights might also reserve big surprises and force us to go beyond such scenario, either by adding new neutrino states, or new interactions, or both.

Acknowledgments

This work is supported by the Italian Ministero dell'Istruzione, Università e Ricerca (MIUR) and Istituto Nazionale di Fisica Nucleare (INFN) through the "Astroparticle Physics" project.

References

1. Review of Particle Physics, S. Eidelman *et al.*, Phys. Lett. B **592**, 1 (2004).
2. Z. Maki, M. Nakagawa, and S. Sakata, Prog. Theor. Phys. **28**, 870 (1962); B. Pontecorvo, Zh. Eksp. Teor. Fiz. **53**, 1717 (1968) [Sov. Phys. JETP **26**, 984 (1968)].
3. L. Wolfenstein, Phys. Rev. D **17**, 2369 (1978); S. P. Mikheev and A. Yu. Smirnov, Yad. Fiz. **42**, 1441 (1985) [Sov. J. Nucl. Phys. **42**, 913 (1985)].
4. J. N. Bahcall, *Neutrino Astrophysics* (Cambridge University Press, Cambridge, 1989).
5. Homestake Collaboration, B.T. Cleveland *et al.*, Astrophys. J. **496**, 505 (1998).
6. Kamiokande Collaboration, Y. Fukuda *et al.*, Phys. Rev. Lett. **77**, 168, 3 (1996).
7. SAGE Collaboration, J.N. Abdurashitov *et al.*, J. Exp. Theor. Phys. **95**, 181 (2002).
8. GALLEX Collaboration, W. Hampel *et al.*, Phys. Lett. B **447**, 127 (1999).
9. GNO Collaboration, M. Altmann *et al.*, Phys. Lett. B **616**, 174 (2005).
10. SK Collaboration, M.B. Smy *et al.*, Phys. Rev. D **69**, 011104 (2004).
11. SNO Collaboration, S.N. Ahmed *et al.*, Phys. Rev. Lett. **92**, 181301 (2004).
12. SNO Collaboration, B. Aharmim *et al.*, nucl-ex/0502021.
13. K. Miknaitis, these Proceedings.

14. KamLAND Collaboration, K. Eguchi *et al.*, Phys. Rev. Lett. **94**, 081801 (2005).
15. B. Berger, these Proceedings.
16. Super-Kamiokande Collaboration, Y. Ashie *et al.*, hep-ex/0501064.
17. L. Sulak, these Proceedings.
18. MACRO Collaboration, M. Ambrosio *et al.*, Eur. Phys. J. C **36**, 323 (2004).
19. Soudan 2 Collaboration, M. Sanchez *et al.*, Phys. Rev. D **68**, 113004 (2003).
20. K2K Collaboration, E. Aliu *et al.*, Phys. Rev. Lett. **94**, 081802 (2005).
21. C. Mariani, these Proceedings.
22. CHOOZ Collaboration, M. Apollonio *et al.*, Eur. Phys. J. C **27**, 331 (2003).
23. K. Eitel, in *Neutrino 2004*, Nucl. Phys. B (Proc. Suppl.) **143** (2005), 197.
24. S.R. Elliott and J. Engel, J. Phys. G **30**, R183 (2004).
25. S. Capelli, these Proceedings.
26. W. Hu, D.J. Eisenstein, and M. Tegmark, Phys. Rev. Lett. **80**, 5255 (1998).
27. WMAP Collaboration, C.L. Bennett *et al.*, Astrophys. J. Suppl. **148**, 1 (2003).
28. SDSS Collaboration, M. Tegmark *et al.*, Phys. Rev. D **69**, 103501 (2004).
29. U. Seljak *et al.*, astro-ph/0407372.
30. S. Pastor, these Proceedings.
31. H.V. Klapdor-Kleingrothaus *et al.*, Phys. Lett. B **586**, 198 (2004).
32. G.L. Fogli, E. Lisi, A. Marrone, and A. Palazzo, hep-ph/0506083, invited review submitted to Progress in Particle and Nuclear Physics (2005).
33. B. Kayser, these Proceedings.
34. G. McGregor, these Proceedings.
35. LSND Collaboration, A. Aguilar *et al.* Phys. Rev. D **64**, 112007 (2001).
36. G. L. Fogli, E. Lisi and A. Palazzo, Phys. Rev. D **65**, 073019 (2002).
37. J. Lesgourgues, S. Pastor and L. Perotto, Phys. Rev. D **70**, 045016 (2004).
38. G. L. Fogli, E. Lisi, A. Palazzo and A. M. Rotunno, hep-ph/0505081.
39. G. L. Fogli, E. Lisi, A. Marrone, A. Melchiorri, A. Palazzo, P. Serra, and J. Silk, Phys. Rev. D **70**, 113003 (2004).
40. M. Maltoni, T. Schwetz, M. A. Tortola and J. W. F. Valle, New Journal of Physics **6**, 122 (2004); S.T. Petcov, ibidem, p. 109; J.N. Bahcall and C. Pena-Garay, ibidem, p. 63.
41. S.M. Bilenky, C. Giunti, J.A. Grifols and E. Masso, Phys. Rept. **379**, 69 (2003).
42. M.C. Gonzalez-Garcia and Y. Nir, Rev. Mod. Phys. **75**, 345 (2003).
43. V. Barger, D. Marfatia and K. Whisnant, Int. J. Mod. Phys. E **12**, 569 (2003).
44. A.B. McDonald *et al.*, Rev. Sci. Instrum. **75**, 293 (2004).
45. S. Goswami, in *Neutrino 2004*[23], p. 121.
46. A.Yu. Smirnov, in the Proceedings of the 2nd International Workshop on Neutrino Oscillations in Venice (Venice, Italy, 2003), hep-ph/0402264.
47. A. Strumia and F. Vissani, hep-ph/0503246.
48. O. L. G. Peres and A. Y. Smirnov, Phys. Lett. B **456**, 204 (1999); O. L. G. Peres and A. Y. Smirnov, Nucl. Phys. B **680**, 479 (2004).
49. M. C. Gonzalez-Garcia and M. Maltoni, Eur. Phys. J. C **26**, 417 (2003).
50. See the contributions at the RCCN Workshop: www-rccn.icrr.u-tokyo.ac.jp/rccnws04
51. M. C. Gonzalez-Garcia, M. Maltoni and A. Y. Smirnov, Phys. Rev. D **70**, 093005 (2004).
52. P. Huber, M. Maltoni and T. Schwetz, Phys. Rev. D **71**, 053006 (2005).
53. M. Tanimoto, these Proceedings.
54. M. Frigerio, these Proceedings.
55. V. A. Rodin, A. Faessler, F. Simkovic and P. Vogel, nucl-th/0503063.
56. 2dF GRS Collaboration, W.J. Percival *et al.*, MNRAS **327**, 1297 (2001).
57. SDSS Collaboration, P. McDonald *et al.*, astro-ph/0405013.

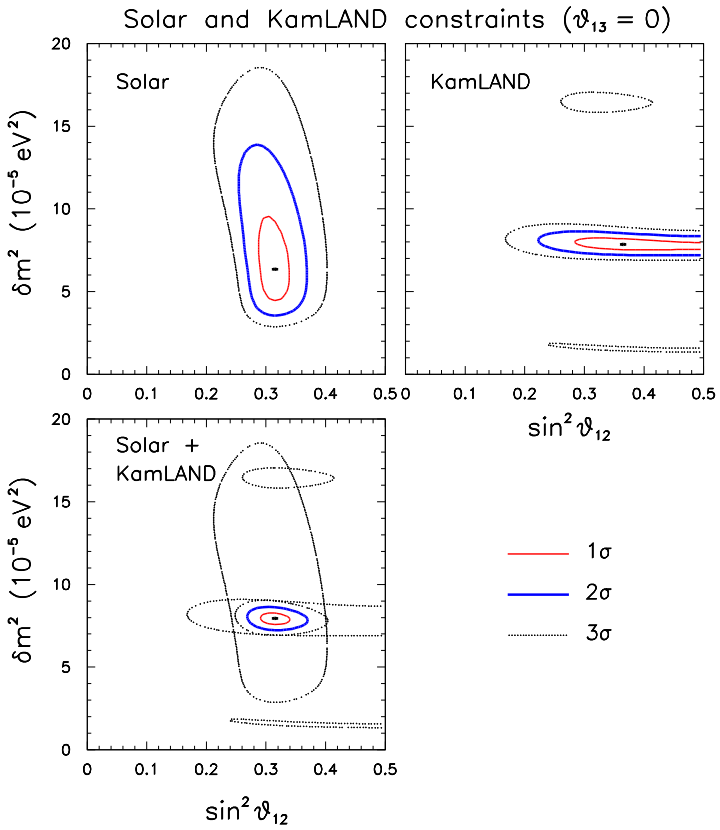

Figure 1: Solar and KamLAND constraints in the mass-mixing plane $(\delta m^2, \sin^2\theta_{12})$ and for $\theta_{13} = 0$, shown both separately and in combination, at 1, 2, and 3σ level.

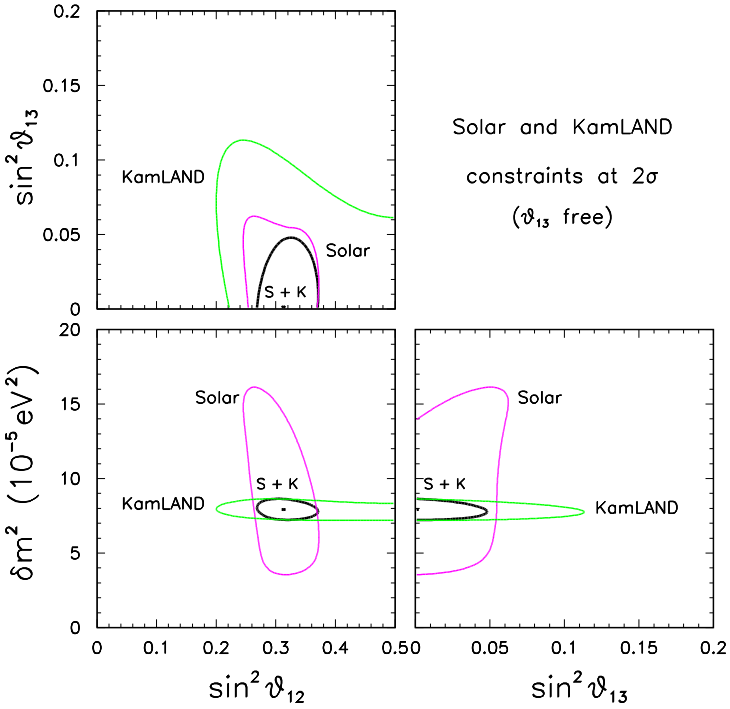

Figure 2: Three flavor analysis of solar and KamLAND data (both separately and in combination) in the parameter space $(\delta m^2, \sin^2\theta_{12}, \sin^2\theta_{13})$. The contours represent projections of the region allowed at 2σ $(\Delta\chi^2 = 4)$.

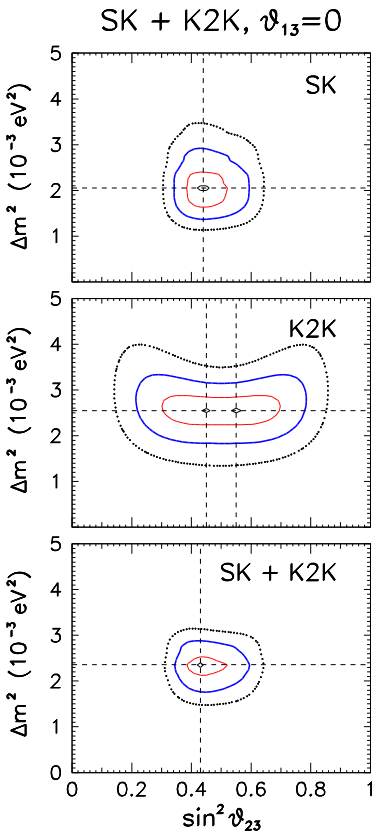

Figure 3: Analysis of SK and K2K data (both separately and in combination) in the plane $(\Delta m^2, \sin^2\theta_{23})$ at $\theta_{13} = 0$. The parameters $(\delta m^2, \sin^2\theta_{12})$ have been fixed at their best-fit LMA values.

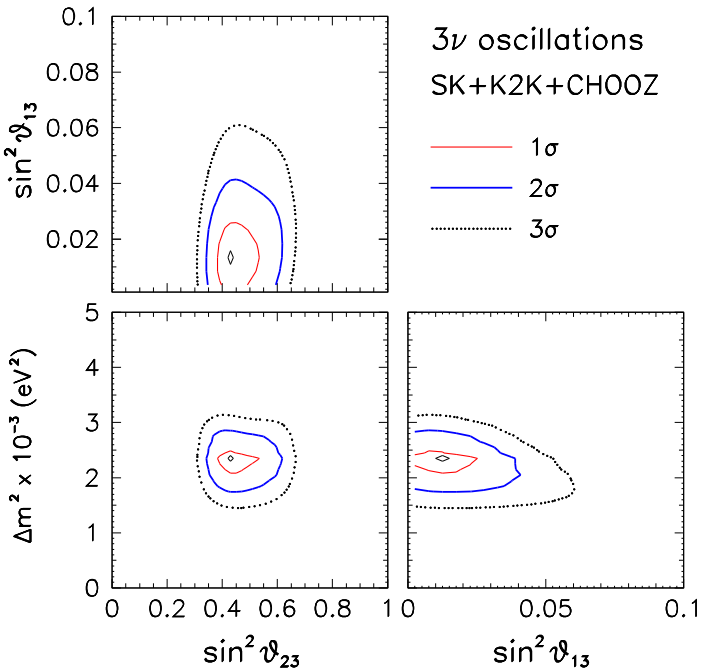

Figure 4: Three-neutrino analysis of SK+K2K+CHOOZ data, including subleading LMA effects. The results are shown as projections of the $(\Delta m^2, s^2_{23}, s^2_{13})$ allowed regions (at 1, 2, and 3σ), marginalized with respect to the four cases $[\cos\delta = \pm 1] \otimes [\mathrm{sign}(\pm\Delta m^2) = \pm 1]$.

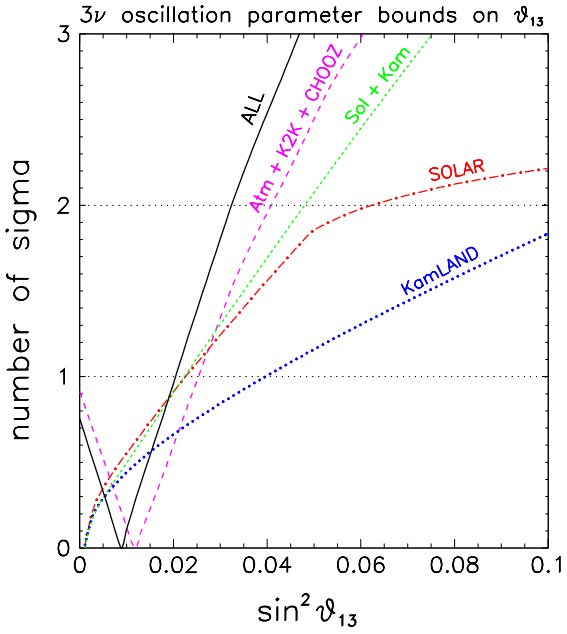

Figure 5: Global three-neutrino analysis of oscillation data. Bounds on s^2_{13} are shown in terms of $n\sigma = \sqrt{\Delta\chi^2}$ for KamLAND (dotted curve), solar (dot-dashed curve), solar+KamLAND (short-dashed curve), SK+K2K+CHOOZ (long-dashed curve) and all data combined (solid curve). In each case, the continuous parameters $(\Delta m^2, s^2_{23}, s^2_{13})$ and—if applicable—the discrete parameters $[\cos\delta = \pm 1] \otimes [\mathrm{sign}(\pm\Delta m^2) = \pm 1]$ are marginalized away.

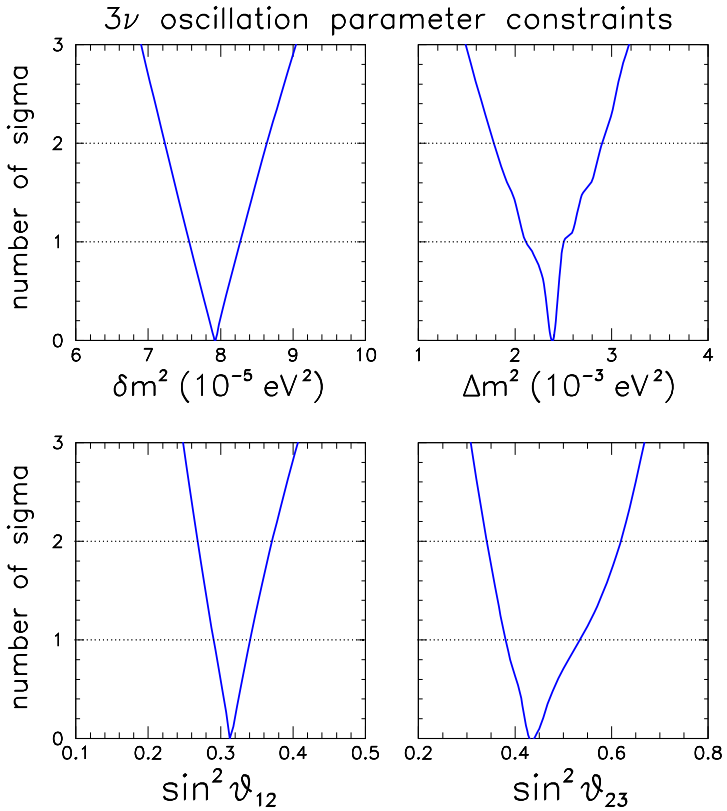

Figure 6: Global three-neutrino analysis of oscillation data. Bounds on each of the parameters δm^2, Δm^2, $\sin^2\theta_{12}$, and $\sin^2\theta_{23}$ are shown in terms of $n\sigma = \sqrt{\Delta\chi^2}$. In each plot, all parameters but the one in abscissa are marginalized away.

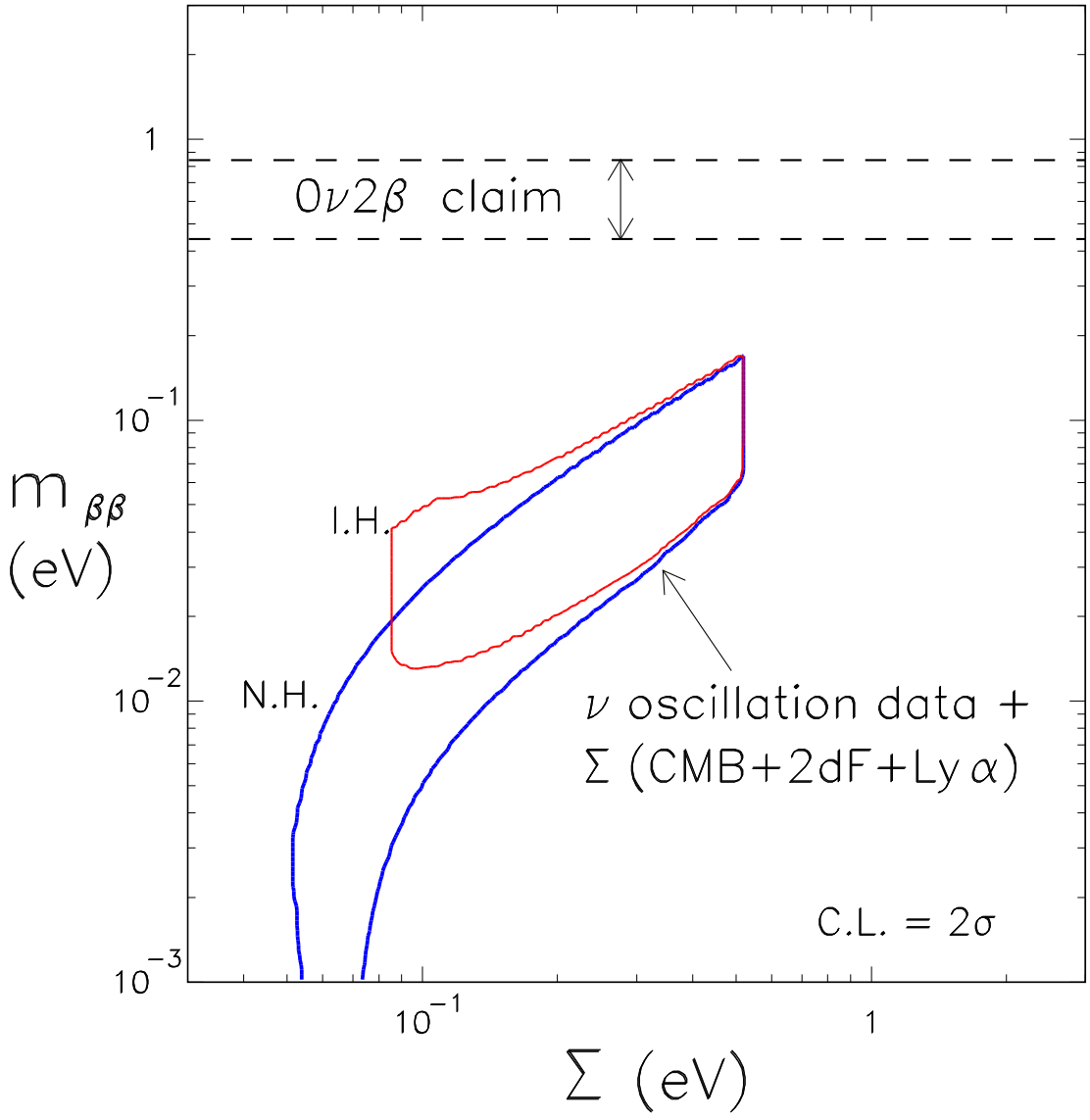

Figure 7: Analysis of oscillatory and non-oscillatory observables in the plane $(m_{\beta\beta}, \Sigma)$. The 2σ horizontal band is preferred by the positive $0\nu 2\beta$ claim, while the slanted 2σ regions below (for normal hierarchy, N.H., and inverted hierarchy, I.H.) are preferred by all other data (i.e., oscillation plus cosmological data). The absence of overlap indicates tension among the data in the sub-eV range, as far as the standard three-neutrino framework is assumed. See also Refs. [32,39]